# An Integrated Health Management and Prognostic Technology for Composite Airframe Structures

**Ingolf Mueller** [1], **Cecilia Larrosa** [1], **Surajit Roy** [1], **Amrita Mittal** [1]
**Kuldeep Lonkar** [1], **and Fu-Kuo Chang** [1]

[1] *Department of Aeronautics and Astronautics, Stanford University,*
*Durand Building, 496 Lomita Mall, Stanford, CA 94305, USA*
{*imueller, clarrosa, fkchang*}*@stanford.edu*

## ABSTRACT

Next generation technology of integrated health management systems for air-transportation structures will combine different single SHM methods to an overall system with multiple abilities considering different stages of damage initiation and propagation. The fundamental configuration of the proposed SHM technique will involve the idea of an integrated passive/active monitoring and diagnostic system extended by numerical modules for lifetime prediction. The overall system is capable of providing real-time load monitoring and damage estimation on a global structure level as well as precise damage diagnostics on a local level. This robust diagnostic technique provides quantifiable damage location and size estimation that account for the uncertainties induced by the environments or the system itself continuously during flight. Additionally, efficient prediction and prognostic methods are integrated with monitoring and diagnostic outputs to provide real time estimation of possible damage scenarios, residual strength, and remaining useful life of the damaged structure. From this result information is gained which allow appropriate preventative actions on the monitored structure. To achieve those objectives, a built-in sensor/actuator network is employed and numerical simulation methods of damage estimation and propagation are developed and applied. The goal of this work is to integrate all these single techniques and subsystems into an integrated structural health management system for composite airframe structures. The system design, data exchange between the different subsystems, and the performance of each module is presented.



## 1 INTRODUCTION

Structural design of air transportation systems includes many goals: light weight for fuel efficiency, stiffness and strength for an appropriate dynamic performance. Another major task is the improvement of the safety of those systems by inspecting for system and component failure. At the same time the downtime of the transportation system due to inspection should be dramatically reduced by nearly continuous monitoring of the structure.

One of the most critical concerns is the presence of undetectable damage, which may be introduced during the manufacturing process as well as in-service events, such as impact loads or fatigue. The presence of any degradation, which is not easily detectable by visual inspection, may significantly reduce the mechanical properties of a component, in particular strength and stiffness. Due to this fact, the design of air transportation systems and associated maintenance practice must take this concern seriously into consideration in practice.

Due to the increasingly high demands for safety and low cost maintenance, the use of a built-in real-time structural health monitoring (SHM) system for aircraft health monitoring is becoming more and more attractive. Unlike traditional NDE systems, the SHM system is designed to apply to a specific structure with a built-in network of sensors and actuators.

Although many well-established diagnostic techniques and prognostic methods have been proposed in the literature during the last decade, each single technology of structural health monitoring aims at observing very specific properties of structures or systems. Due to this fact, the performance of a single technology is subjected to inherent limitations of the applied methodology and may only cover single aspects of structural health monitoring. In an effort to improve the overall system performance and to merge interactively the capabilities and advantages of the several single methods, research effort is conducted to link and to integrate different SHM technologies to a complete system for the purpose of an Integrated Vehicle Health Management (IVHM) as required for next-generation air and space transportation systems. The goal of

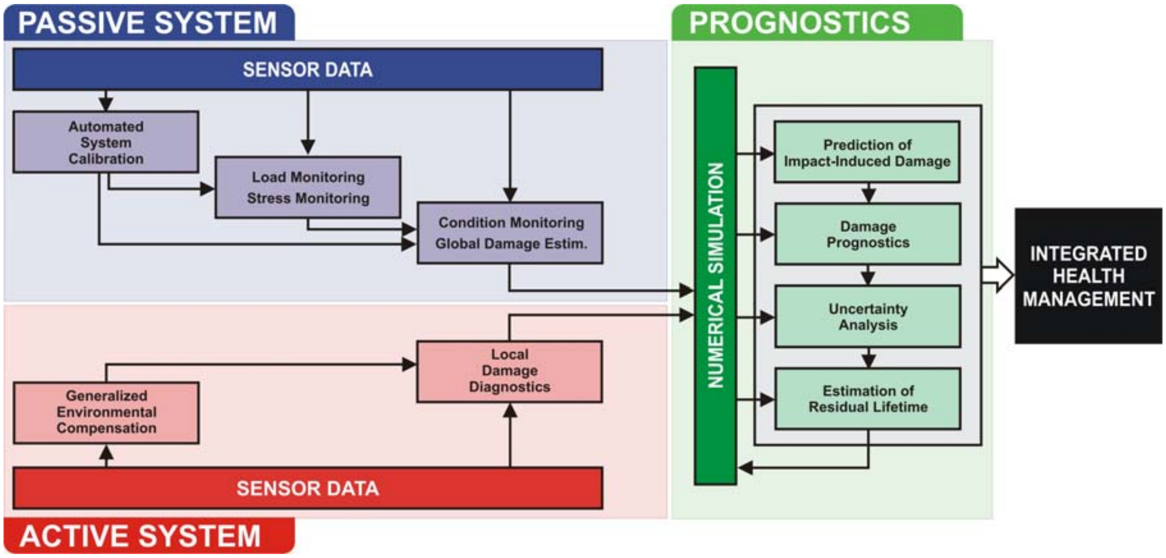


Figure 1: Flowchart of the interactive health management system as proposed.

IVHM is to develop validated technologies and techniques for automated detection, diagnosis and prognosis to enable early detection and mitigation of adverse events during flight. Adverse events include those that arise from system or component faults or failures due to damage, degradation, or environmental hazards that occur during service of vehicles. The capabilities of the IVHM systems will comprise rapid detection and diagnosis of adverse events, estimation of severity and remaining useful life (RUL) for the affected systems. The gained health information will be distributed to other subsystems as real-time automated reasoning and decision making systems. The integration of monitoring and diagnostics with damage prediction and prognostics into a health management system is still a very challenging technical task and the subject of the current research. In particular, the exchange and the transfer of health data between the different subsystems as well as an efficient interaction to achieve optimal performance need to be explored in detail and receive immerged attention. The details of data flow and linkage between the subsystems are illustrated by the flowchart of Figure 1.

After final completion, the proposed technology will be capable to diagnose automatically in real-time the health condition of a structure as well as provide an estimate of the residual strength and remaining useful lifetime to optimize the performance and off-service schedule of the transportation system. Accordingly, the health management system relies on a network of sensors and actuators to be integrated with the structure and be equipped with a diagnostic capability for detecting damage and a prognostic capability to predict the residual life of the damaged structures in service.

By merging all the aforementioned single techniques and subsystems an integrated structural health management system for composite airframe structures is obtained having unique capabilities of interactive monitoring, detection and prediction.

After a short introduction of the embedded network technology, each major SHM subsystem is briefly described along with interfaces to the linked subsystems. The current state of work and open questions are discussed.

## 2 PASSIVE AND ACTIVE MODE OF EMBEDDED SENSING NETWORKS

Structural health monitoring techniques require the use of built-in sensors in a network to monitor external conditions and structural integrity. In general, there are two types of sensor-based diagnostic and monitoring systems: *passive sensing* (e.g. (Doyle, 1987; Yen *et al.*, 1994; Jiang *et al.*, 1998; Fogg *et al.*, 1993; Seydel and Chang, 1999; Chang and Seydel, 2001; Park, 2005; Markmiller, 2007)) and *active sensing* (e.g. (Chang and Beard, 1997; Chang and Roh, 1995; Chang and Ihn, 2004)). In the majority of cases, piezoelectric sensors are employed to build sensing networks. Piezoelectric sensors are active transducers, which can act for both the collection of measurement data at certain points of the structure and the generation of controlled diagnostic signals.

A passive system is useful to monitor changes in the environment, such as loads and impacts, but it is extremely difficult to locate damage or cracks with high reliability and good resolution. However, innovative passive technologies may have the capability to provide information on a global structure level about the existence and rough location of damage, which might be considered within a global condition monitoring process. Since no actuators are needed here (only operational excitation is used) a limited hardware is sufficient to operate the system. For the proposed health management system, the passive network technology will mainly be used to acquire real-time sensor data for impact monitoring as one crucial SHM subsystem.

Re-examination and interrogation in order to locate and characterize damage, as well as to estimate the residual life of structures, becomes possible within an

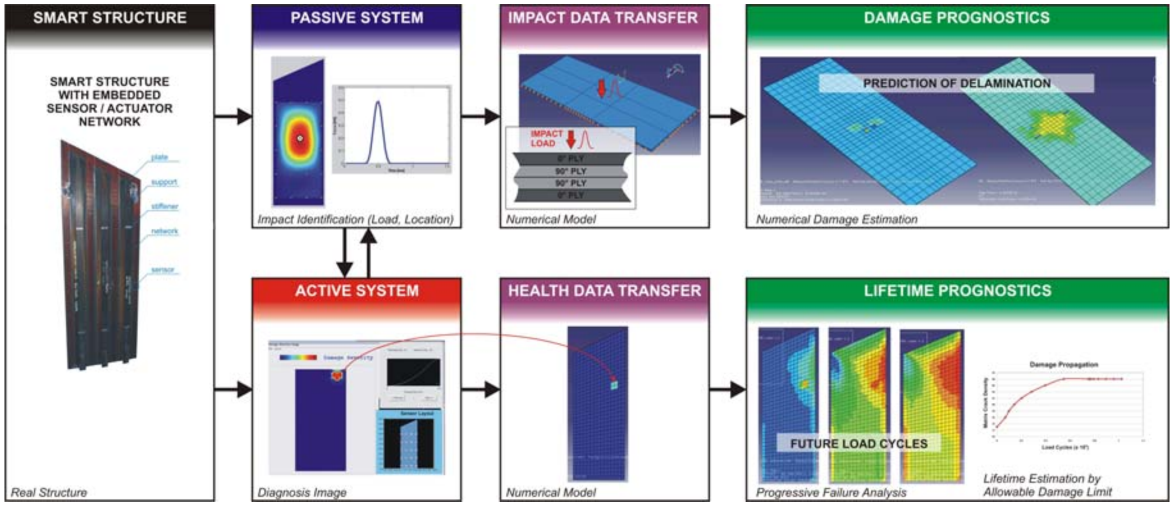


Figure 2: Capabilities and flow of structural health data of the interactive health management system.

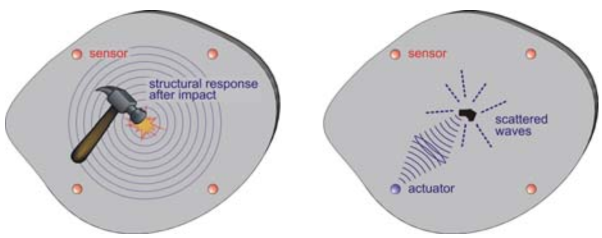


Figure 3: Passive (left) and active sensing networks (right).

active sensing approach. In principle, an active system allows damage to be interrogated by injecting controlled diagnostic signals (i.e. guided Lamb waves) into the structure. With the known inputs, the changes in local sensor measurements are associated with the introduction of damage in the structure. Here, the active sensing approach compares the sensor data before and after an event to interrogate the structural condition. Therefore, it is most effective to detect damage and local defects in structures. Although these techniques have been demonstrated to be a promising method for reliable damage diagnostics, active systems have the disadvantage that extensive hardware and power supply is needed to operate the system. Additionally, the installation of active networks may not be feasible on the entire structure and usually only monitoring of structural hot-spots is performed.
Current research, as described in this contribution, aims to link the two sensing technologies in an effective way which allows to merge the capabilities and advantages of the two sensing technologies. The passive technology constantly monitors the structure and associated algorithms will provide real-time capabilities (Park, 2005), (Markmiller, 2007) for global impact and condition monitoring. After detection of a severe impact event, data of impact location and impact force history will be submitted to a damage prediction module where numerical simulation is used to estimate the impact damage by failure analysis. Additionally, the active technology provides the damage diagnostics and will afterwards interface with numerical prognosis module for estimation of remaining useful lifetime.
In summary, the uniqueness of this approach is an interactive global-local diagnostics by integration of passive sensor data as well as active sensor data provided by locally built-in actuators in the structure. The overall system will be capable of providing real-time load monitoring on a global structure level as well as precise damage diagnostics on a local level. For this purpose, structural health data will be exchanged between the subsystems and numerical models will be continuously updated with occurring degradation.

## 3 IMPACT MONITORING BY PASSIVE SENSING NETWORKS

Real-time impact monitoring is an important key approach for structural health management. For this purpose, a passive sensing network based on built-in sensor technology is employed to acquire local sensor data of structural response due to impact events. However, passive sensing approaches rely on numerical models to reconstruct meaningful information as impact location and impact load history from the point-wise sensor data.
Generally speaking, recovering external impact loads using structural response data works on the principle of an inverse problem (see Figure 4). While the phenomenon of interest (impact location and force history) may not be measured directly, there exists some other variable that can be observed (sensor data of structural response), which is related to the event of interest through the use of a data-derived computer model. Depending on its mathematical representation, the properties of the adopted model, and the sensor network configuration (number and location of sensors) the resulting inverse problem may be subjected to the difficulties of ill-posedness. According to Hadamard (Hadamard, 1923), the ill-posed properties of the resulting inverse problem appear in terms of stability, existence, and uniqueness of the solution and may cause serious errors in the identification re-

sults. The effect of ill-posedness for the problem of impact monitoring has been studied in (Mueller and Chang, 2009), in particular with a view to influence of the sensor network configuration.

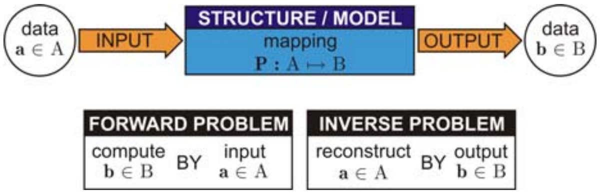


Figure 4: Schematic of inverse problems.

Several models and techniques (e.g. (Doyle, 1987; Yen *et al.*, 1994; Jiang *et al.*, 1998; Fogg *et al.*, 1993; Seydel and Chang, 1999; Chang and Seydel, 2001; Park, 2005; Markmiller, 2007)) have been proposed in the literature to identify impact events from passive sensor data. Park and Chang (Park, 2005) have proposed an advantageous methodology which is based on a linear system identification model. This autoregressive model with exogenous input (ARX) (Ljung, 1999) is a linear finite difference model which represents the dynamic response of a linear elastic structure by a parametric approach as given by equation 1.

$$\varepsilon(k) = \sum_{i=1}^{n} a_i \, \varepsilon(k-i) + \sum_{j=1}^{m} b_j \, f(k-j) \qquad (1)$$

Here, $\varepsilon(k)$ and $f(k)$ are a sequence of strain and impact force values at discrete time instances. The parameters $a_i$ and $b_j$ are the ARX parameters of the model while $n$ and $m$ represent the order of the model, respectively. A training step is needed to find appropriate ARX parameters based on the physical behavior of the structure. For this purpose, sets of training data in terms of impulse response are generated and ARX parameters are derived.

For the inverse reconstruction of the impact force history the ARX model need to be inverted. One striking feature of ARX based methods is that the inversion can be performed analytically as shown by Park (Park, 2005). Due to this fact, real-time capabilities of impact monitoring module are achieved. Furthermore, this method can be applied to complex structures with uncertain properties and boundary conditions. On the other hand, the proposed ARX model has inherent assumptions of linearity. Non-linear structural behavior as occurring on time-variant structures (e.g. damage propagation) may not be represented correctly. For these cases, a model update or the utilization of another set of ARX parameters might be necessary to capture appropriately the current condition of the structure. Hence, a feed-back of the current health status received from active diagnostics is needed to involve the latest structural condition.

Figure 5 illustrates the results of the impact monitoring system on the example of a stiffener panel manufactured by Boeing Company (also see Figure 14). The proposed method identifies the impact location as well as the impact load history in real-time. As a comparison, the impact force was directly measured by utilization of a modal hammer (red curve) and reconstructed by the described ARX approach (blue curve). As can be seen, the results are in a good agreement.

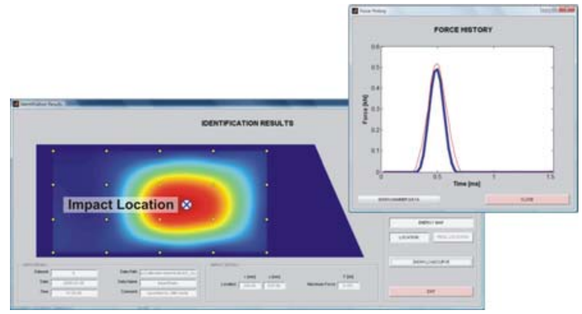


Figure 5: Results of impact monitoring on the example of a composite stiffener panel (left: impact location and energy map, right: impact force history).

### 3.1 Stability of ARX Models for Impact Monitoring

One significant difficulty in parametric identification of ARX models is an appropriate assumption for the model order $n$ (see Equation 1) to construct the regression vector. In fact, an incorrect choice for the model order $n$ will lead, in general, to difficulties in terms of model accuracy.

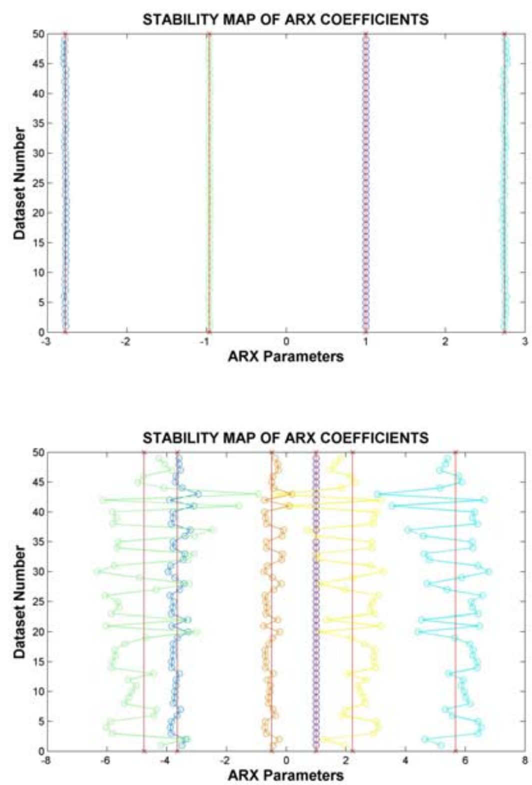


Figure 6: Stability map of ARX models for different model orders $n$ (upper: $n = 3$, lower: $n = 5$).

Selecting a value for $n$ too large is called over-parametrization and may lead to unstable ARX estimates in the majority of cases. On the other hand, selecting a value $n$ too small will lead to mismatch between measured data and model output. In this case, errors of approximation may be large. A heuristic approach for estimation of an appropriate model order can be found in (Park, 2005).
In order to evaluate the model order for a given structure a stability map for the estimated ARX parameter can be compiled. It can be expected that almost identical or similar impact events will only lead to slight changes for the estimated ARX parameters. Such a stable behavior can only be found for appropriate model orders $n$. In all other cases, the model might be subjected to instability and, hence, slight changes in the input/output data leads to large differences in the computed ARX parameters (fluctuations).
Practically, a large number of input/output data will be recorded based on impacts at the same location and with similar amplitudes (impact force). For each set of I/O data an estimation of ARX parameters is performed and results are collected in a stability map (see Figure 6). For stable model orders n straight lines for the ARX parameter are obtained. Figure 6 shows a typical result on the example of the before-mentioned composite stiffener panel. A model order $n = 3$ (upper) will show stable ARX models while a 5th order model (lower) leads to strong parameter fluctuations. As a result of extensive experimental tests, it has turned out that model order $n = 3$ is the most appropriate assumption for the considered class of structures.

### 3.2 Automated System Calibration and Simulation-Based Training of ARX Models

In order to improve and to speed up the necessary training step for the ARX model Markmiller and Chang (Markmiller, 2007) recently proposed the utilization of a structural model based on Finite Element methods to obtain numerically the necessary impulse responses of the structure. Figure 7 shows the two-stage approach in a schematic.

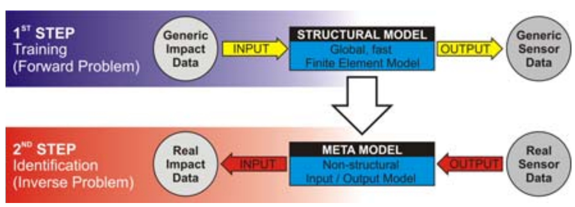


Figure 7: Training of ARX models by numerical simulation.

Apparently, the quality of the training process strongly depends on the accuracy of the Finite Element model employed during the training process. Stated another way, without having a reliable simulation model at hand, the training step of finding appropriate ARX parameters may lead to incorrect results. Thus, the calibration of the numerical model and the sensor / model relations is of immense importance.
The calibration of the sensor/model relation involves usually extensive experimental testing which might be difficult, time-consuming, and expensive for large-scale structures. In particular with a view to future large sensor networks – having potentially thousands of sensors in a network – a reliable and efficient calibration technique is strongly required.
A promising alternative to extensive experimental lab tests is to extract the necessary dynamic properties for the numerical model from the structure response collected by the passive network during operation (operational data / in-flight data) or noise tests (Chang *et al.*, 2008). Here, the challenge appears in the reliable extraction of needed system properties (system identification) from sensor data only (dynamic response) while the ambient input (dynamic excitation) is not or not completely known. In contrast, commonly applied procedures of system identification are based on input/output relations. Nevertheless, the key target of both approaches is the same, namely to get knowledge either of frequency response or impulse response functions of the system under consideration. The obtained data are either used to update the numerical model in terms of model calibration or provide a direct basis for the training process.

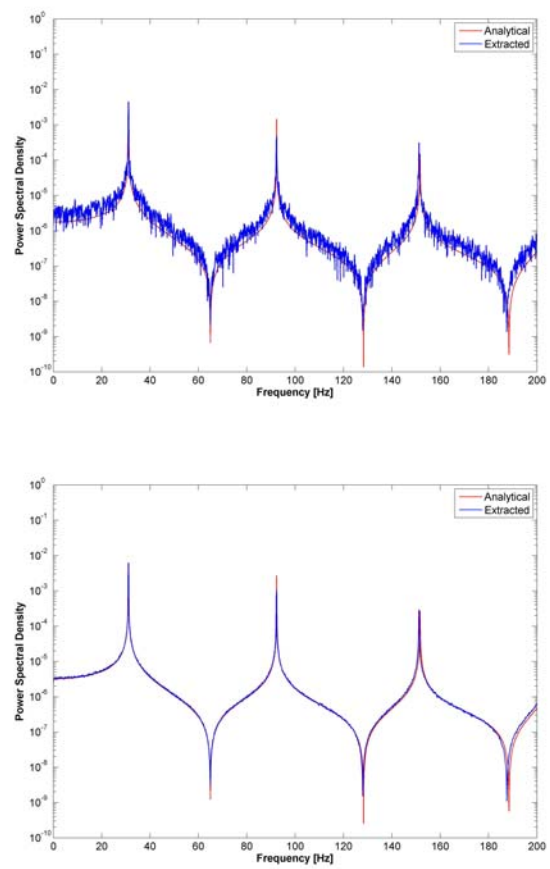


Figure 8: Extracted vs. analytical frequency response for the example of a beam-type structure (upper: after 200 sec measuring time, lower: after 2000 sec measuring time).

In general, the methodology of output only system analysis - as core for automated sensor / model calibration - is based on three foundations: (1) long-term measurements with appropriate sampling rate by the passive sensing, (2) averaging in order to reduce measuring noise and random effects, and (3) power spectral density estimate. Following the assumption that the natural (operational) excitation of a flexible structure is characterized by continuous energy supply with a broad spectrum, one can expect energy to concentrate around modal frequencies. Hence, a power spectral density estimate will lead to the according frequency response function that can be utilized for a subsequent model updating process or direct training step. Figure 8 shows an example for the reconstruction of frequency response functions by output-only analysis as part of the proposed calibration method.

## 4 DAMAGE PREDICTION AFTER IMPACT DETECTION BY PASSIVE SENSING NETWORKS

To accomplish the goal of a health management system with immediate capabilities for damage prediction after an adverse impact event, the results of impact monitoring will be linked with numerical failure analysis. Once the impact load history is known by the impact monitoring system, an appropriate FE model for the structure is employed to obtain the stresses during the impact event. The damage will then be estimated from the stresses using appropriate failure criteria. In this research, criteria for matrix cracking and delamination have been considered and implemented.

A lot of research has been conducted during the past decades to investigate the type, location and the extent of damage in the fiber reinforced laminated composites due to impact events. As commonly acknowledged, transverse low velocity impact on laminated composites mainly induces intra-ply matrix cracking and inter-ply delaminations (Choi, 1990; Wu and Springer, 1988; Wu and Chang, 1989; Geubelle and Baylor, 1988). The occurrence of cracks is primarily due to the inter-laminar transverse shear stress and transverse in-plane stress. Delamination growth at the interface is governed by the state of stresses of the constraining plies or ply groups having different orientations. Many researchers have developed analytical models to estimate the type and extent of damage due to the low velocity impact forces. A detailed investigation on the actual modes and mechanisms of impact induced damage on the laminated composites was presented by Choi (Choi, 1990).
The analytical model for predicting the delamination in the composite structures comprises first carrying out a transient dynamic analysis under the application of the load history obtained from the integrated passive system and subsequently applying appropriate failure criteria (Choi, 1990), (Hashin, 1980) to capture the initiation sites and the extent of damage. The transient dynamic analysis of a composite structure is performed using the commercial Finite Element package ABAQUS along with a UMAT user-defined material subroutine. Once the stresses are obtained the following criterion is employed to predict the occurrence of matrix cracking

$$\left(\frac{\sigma_{yy}}{Y_t}\right)^2 + \left(\frac{\sigma_{yz}}{S_i}\right)^2 \geq 1 \tag{2}$$

where $x$, $y$ and $z$ are the principal material directions of the laminate. Here, $Y_t$ is the in-situ transverse tensile strength and $S_i$ is the in-situ ply transverse shear strength. Both these strength parameters depend on the relative thickness and the orientation of the constraining ply-groups. These strength parameters are determined from the empirical relationship as found in the literature (Lessard, 1989).

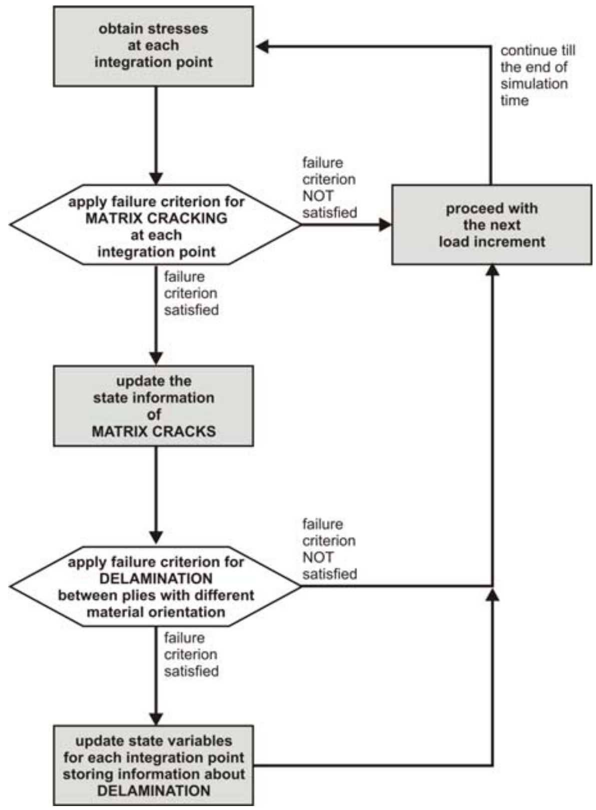


Figure 9: Flowchart for predicting the extent of delamination under a given impact load.

Once the matrix failure criteria is satisfied at a particular material point in any ply group near the interface of the two different ply-groups (having different material orientations) then for all the subsequent time steps of the dynamic analysis the possible occurrence of delamination and its growth is monitored. The following criterion (Choi, 1990) is used to estimate the presence of delamination

$$D_a \left[ {}^{\langle n \rangle}\left(\frac{\sigma_{yz}}{S}\right)^2 + {}^{\langle n+1 \rangle}\left(\frac{\sigma_{xz}}{S}\right)^2 + {}^{\langle n+1 \rangle}\left(\frac{\sigma_{yy}}{Y}\right)^2 \right] \geq 1 \tag{3}$$

where $n$ denotes the upper layer and $n+1$ the lower layer of the interface. The stresses $\sigma_{yz}$ and $\sigma_{xz}$ represent inter-laminar shear stresses while $\sigma_{yy}$ is the transverse stress in a ply. Again, $Y$ denotes the transverse

strength and $S$ represents the shear strength. The factor $D_a$ is an empirical constant which has to be determined by experiments. For graphite epoxy composites T300/976 an average value of $1.8$ has been found in literature. The flowchart of Figure 9 depicts the algorithm which has been implemented in the user-defined subroutine UMAT.
The validation of the UMAT material subroutine which has been developed to predict the location and the extent of the delamination in a ply under a given impact load history is carried out with the experimental results available in the literature (Choi, 1990).

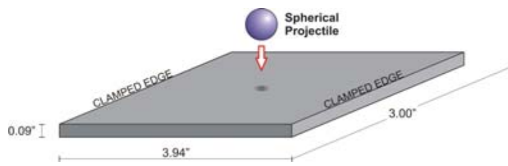


Figure 10: Geometry of the flat plate considered for validation of the implemented UMAT subroutine.

A flat composite laminated plate $3.94" \times 3.00" \times 0.09"$, clamped at the two outer edges was impacted with spherical projectiles directed at the center. A linear 8-noded 3d composite solid brick element (C3D8) is used to model the structure with one integration point along the thickness direction for each ply in the lay-up. The material properties of the plate are shown in the table below (Choi, 1990). The material of the spherical projectile is taken as steel with a mass of $0.353$ lb.

Table 1: Material properties for 'T300-976' as available in the literature.

| Material Property | Symbol [Unit] | Value |
|---|---|---|
| *a) Elastic Constants* | | |
| in-plane longitud. modulus | $E_{xx}[psi]$ | 0.224 E08 |
| in-plane transverse modulus | $E_{yy}[psi]$ | 0.130 E07 |
| in-plane shear modulus | $G_{xy}[psi]$ | 0.995 E06 |
| out-of-plane shear modulus | $G_{yz}[psi]$ | 0.463 E06 |
| in-plane Poisson's ratio | $\nu_{xy}[psi]$ | 0.228 |
| out-of-plane Poisson's ratio | $\nu_{yz}[psi]$ | 0.400 |
| *b) Inertia* | | |
| Density | $\varrho[lbm/in^3]$ | 0.056 |
| *c) Strength* | | |
| longitudinal tension | $X_T[psi]$ | 0.217 E06 |
| longitudinal compression | $X_C[psi]$ | 0.227 E06 |
| transverse tension | $Y_T[psi]$ | 6435.0 |
| transverse compression | $Y_C[psi]$ | 0.360 E05 |
| ply longitudinal shear | $S[psi]$ | 0.145 E05 |

First, a convergence study for the Finite Element model has been carried out to understand the effect of the element size on the plate's central deflection as depicted by Figure 11. In the following a total of $900$ elements is selected for the analysis as result of the mesh convergence study.

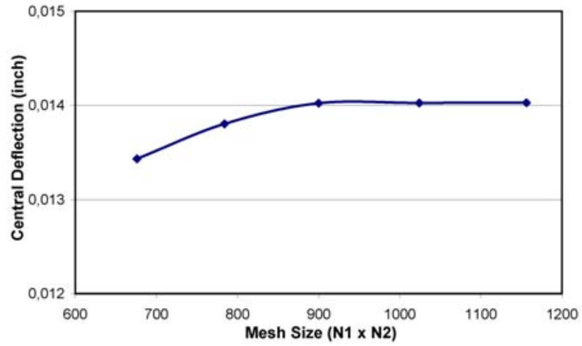


Figure 11: Mesh convergence study for the maximum central deflection of the plate under the specified impact force distribution.

Figure 12 shows the comparison between the predicted and the observed delamination sizes along the interface that has the maximum delamination size in the composite lay-up for different projectile velocities. For a $[-45_4/45_8/-45_4]$ lay-up (Figure 12, top) the maximum delamination size is between the 4th and 5th interface when counted from the bottom ply. The load is applied at the center of the top ply which is defined as the 16th ply. Similarly, for a $[0_4/45_2/-45_4/45_2/0_4]$ lay-up (Figure 12, bottom) the maximum delamination occurs along the 4th and 5th interface located between $0^0$ and $45^0$ ply.

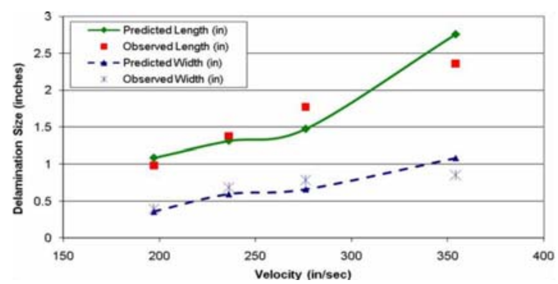


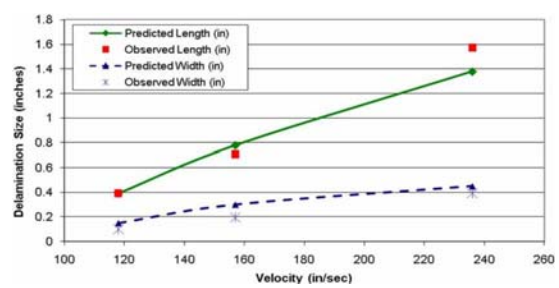


Figure 12: Comparison of the delamination size between the experimental values and predictions from the numerical simulation for T300/976 composite (upper: $[-45_4/45_8/-45_4]$ lay-up, lower: $[0_4/45_2/-45_4/45_2/0_4]$ lay-up).

It can be observed from Figures 12 that the predicted values match well with the experimental observations for the delamination sizes. The method thus developed can be used to predict the delamination in a composite lay-up once the loading history is known from passive load identification.

Figure 13 (top) shows the force history as obtained from a real impact event monitored by the passive system. Following, this impact force history is applied to the failure analysis model in order to predict the damage in terms of delamination. As an example, a flat composite plate $3.0" \times 3.0" \times 0.1"$ clamped at all the edges has been considered and the lay-up being assumed as $[0/{-45}/45/90]_{2S}$. It is observed from the simulations that no damage will occur along any interface for the given loading conditions originally derived from an integrated passive monitoring system. Accordingly, the load history is linearly scaled

$$f^{\star}_{impt}(t) = \alpha \cdot f_{impt}(t) \tag{4}$$

to predict the threshold value of the peak load which will cause the first delamination in any one of the plies of the laminated structure. It is found that the delamination will occur only when the peak load value is increased by factor $\alpha = 3$.

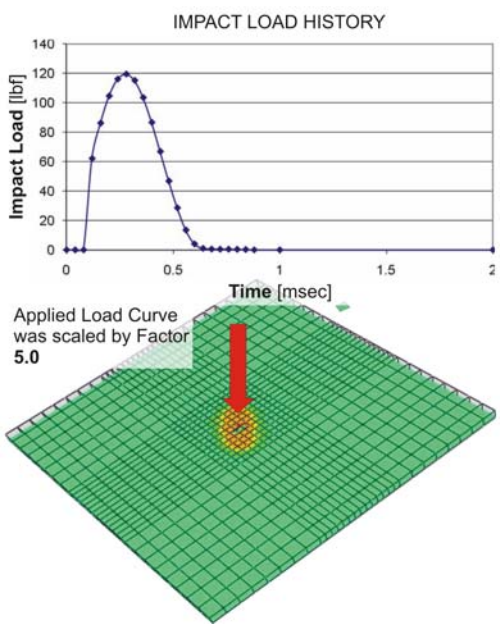


Figure 13: Impact force history as obtained from the integrated passive system (upper); extent of delamination at the 3rd interface for the T300-934 $[0/{-45}/45/90]_{2S}$ composite (lower); note: the impact force history is scaled by factor $\alpha = 5$ with respect to the shown curve as obtained from the integrated passive system (upper) to produce the extent of damage as shown.

Once the impact force distribution on a laminated structure is known, the state of damage in the structure in terms of delamination can be computed. In addition, an estimate of the peak load required to cause the first occurrence of damage in the laminated structure can be predicted. Figure 13 (bottom) depicts the extent of delamination between 2nd and 3rd interface for the T300-934 $[0/{-45}/45/90]_{2S}$ composite when the peak load is increased by a factor of $\alpha = 5$.

In summary, it has been demonstrated that diagnostic load monitoring by passive sensing data with a link to impact damage prediction has great potential for the development of next-generation health management systems. The state of delamination (location and size) in any composite laminate can be evaluated by using the developed material subroutine UMAT in conjunction with the commercial Finite Element package ABAQUS. Future work will be conducted to utilize the damage information thus available to provide a first estimate for the health of the structure in terms of the residual strengths and residual fatigue life.

## 5 ACTIVE SENSING FOR DAMAGE DIAGNOSIS

One of the major advantages sensing networks based on piezoelectric transducers is that it can be used for an active and passive mode. In the active mode, each piezoelectric element in the sensor network can be used as both a transmitter and a receiver so that more comprehensive information about the structure and the damage can be retrieved.

The fundamental principle of damage diagnosis by active sensing is based on the controlled injection of diagnostic waves into the structure under observation. It is widely acknowledged that the utilization of guided Lamb waves is one of the most promising approaches in this area which is increasingly applied in various engineering fields. Some of the fundamental advantages over other methodologies are the capabilities to inspect large structures and the entire cross-section area without disassembling the system under inspection. A comprehensive review of the current state for the guided Lamb wave technique can be found in (Su *et al.*, 2006).

The acousto-ultrasound (AU) technique based on Lamb waves has been demonstrated to be very sensitive and effective in detecting of local damage (Wang and Chang, 2000), (Park and Chang, 2003), (Kim *et al.*, 2008), (Boller *et al.*, 2009), in thin to moderate thick structures which is ideally for aircraft structure application. Advanced diagnostic images similar to ultrasonic images have been developed to identify the location of damage and to estimate its extent.

Although, the damage diagnosis by active sensing has attracted much research effort during the last years and extensive studies have been conducted, still some fundamental difficulties and open questions exist that require pursuing the research efforts. In the following, a question with particular relevance for the proposed interactive health management system has been taken out and will be discussed.

### 5.1 Compensation of Environmental Effects

An active diagnosis system allows damage to be interrogated by injecting controlled diagnostic signals into the structure. With the known inputs, the changes in local sensor measurements (compared to baselines of a pristine state) are associated with the introduction of damage in the structure.

In general, a set of baseline data will be collected from all actuator / sensor paths on the intact structure. The signals will change if any local degradation occurs. To quantify the change in the signals due to damage, the post-damage signal can be subtracted from the original (baseline) signal before there was damage. The remaining difference is called scatter signal that is used to quantify the amount of change in the signal of a particular actuator-sensor path. After data normalization (e.g. taking path length into account) of the scatter signal amplitude, the ratio between signal scatter and signal baseline within a certain time window $[t_0, t_1]$ provides an indicator for structural alteration, as shown by Equation 5.

$$\mathrm{SER} = \left[ \frac{\int_{t_0}^{t_1} \|S_{SC}(\omega_0, t)\| dt}{\int_{t_0}^{t_1} \|S_B(\omega_0, t)\| dt} \right]^n \tag{5}$$

Compiling this information for each sensing path creates the basis for the diagnostic image. Diagnostic imaging which highlights the region where significant changes in sensor-actuator signals occur has been demonstrated to be a beneficial tool for locating damage and potentially quantify the damage.

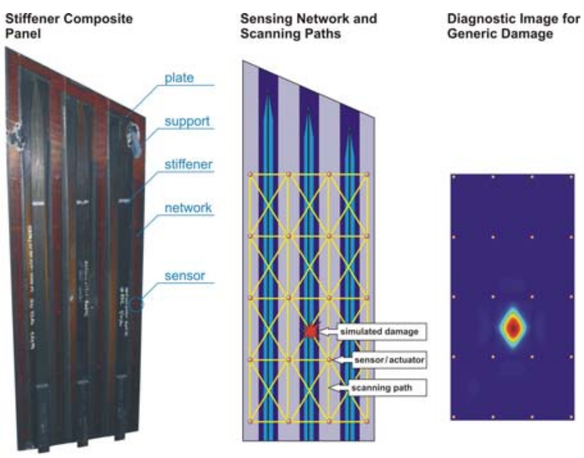


Figure 14: Example of damage diagnosis by guided lamb waves on the example of a stiffener composite panel with generic damage.

However, the acousto-ultrasound technique is not only sensitive to structural alterations as induced by damage, it is also sensitive to the change of environmental condition (Scalea and Salamone, 2009), (Raghavan and Cesnik, 2008). Structures with integrated health monitoring systems operate across a variety of environmental conditions including changes in temperature, pressure, humidity, static load and vibration. The effect of these factors on Lamb wave propagation can easily be interpreted as an indication of structural damage or, stated another way, environmental effects can corrupt the sensor signals in such a way that an accurate prediction of location and size of the damage will not be possible in the majority of cases. Sensor signals change because variation in environment alters material properties of the host structure, PZTs, and the bondline adhesive layer. Hence, in order to avoid false warnings, the SHM technology must be compensated for environmental factors for fielded application.

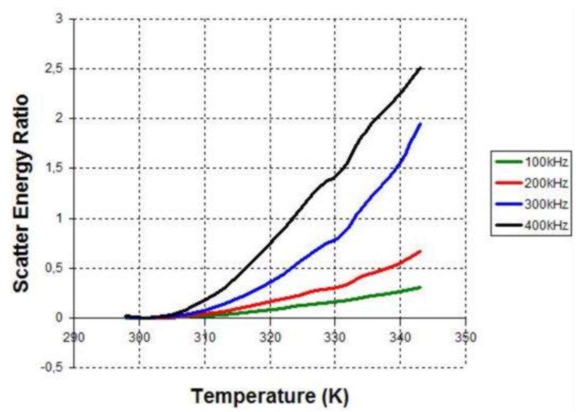


Figure 15: Example for the influence of different environment temperatures to the scatter energy ratio for different scanning frequencies ($100$ kHz ... $400$ kHz).

Current approaches try to overcome these difficulties by utilization of large sets of different baseline data for different environmental conditions to compensate environmental effects on damage diagnosis. Moreover, interpolation techniques are applied to provide baseline data for all possible conditions. However, interpolation in heterogeneous data may be a source for severe errors in damage diagnosis, in particular, if based on a small number of experimental sets of baseline data. On the other hand, the acquisition of a large database for the necessary baseline data might be time-consuming and inefficient even for large structures.

In an effort to improve the current compensation technique research is conducted to develop a method with minimum of necessary baseline data to compensate for the environmental effects on sensor signal. The method to be developed will be based on the physics that causes the environment-induced changes in the diagnostics signals. For this purpose, the physics of wave propagation under certain environmental conditions need to be studied and simulated by numerical analysis.

However, direct relationships between the signal changes and environmental conditions are still quite difficult to establish, and such a relationship may change with sensor/actuator location and structural geometry, etc., making it difficult to quantify and to compensate the environmental effects in a real application.

Currently, numerical tools based on Finite Element methods are developed to achieve reliable simulation for the wave propagation of Lamb waves in structures of practical complexity. The simulation is based on the application of spectral elements (Komatitsch and Vilotte, 1998) within an explicit time integration scheme. This methodology was presented recently by Chang and his associates in (Kim *et al.*, 2008) and turns out to be promising as a fundamental basis for environmental compensation (Ha *et al.*, 2009).

The following study is aimed at understanding the effect of elevated environmental temperature on Lamb wave propagation. Experiments are carried out over temperature range from $25^0$C to $75^0$C where a significant change in sensor signal with temperature is observed. A parametric study is performed by simulation to identify the key parameters that change Lamb wave propagation with temperature and the bondline adhesive is found to be one of the most critical factors.

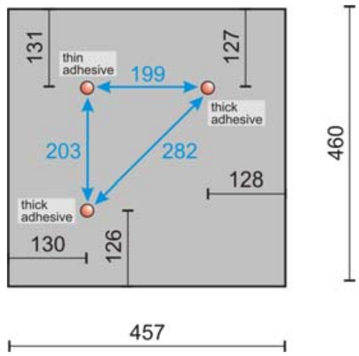


Figure 16: Experimental setup of an aluminum plate with surface mounted PZT transducers (all dimensions are in mm).

An aluminum plate with $0.8$ mm thickness is used to investigate the effect of temperature. Dimensions of the plate are shown in Figure 16. Piezoelectric transducers (PZT 5A) of $0.25$ mm ($10$ mil) thickness and with a quarter inch diameter were glued to the surface using conductive epoxy (Chemtronics cw2400) at locations indicated in Figure 16. The PZTs are glued with varying amount of glue to study whether adhesive thickness affects the Lamb wave propagation with temperature. The specimen is heated in an oven to elevated isothermal temperatures. A *ScanGenie* scanning device from *Acellent Technologies* is employed for data acquisition. Here, a $5$ peak tone burst wave has been selected as actuation input each at $300$ kHz and sensor signals are measured at $25^0$C, $50^0$C, and $75^0$C with $24$ MS/s sampling rate in a pitch-catch mode.
The aforementioned Spectral Element Method (SEM) is employed to simulate the propagation of Lamb waves in the described aluminum plate with surface mounted PZT actuator and sensors. For this purpose, $0.04$ mm and $0.10$ mm thicknesses are assumed for thin and thick adhesive layers respectively.

In general, results of the numerical analysis show a dominant influence to the signal by temperature-induced property changes for the adhesive layer of sensor network. Exemplarily, Figure 17 compares simulation results in terms of time signals for Lamb wave propagation. In order to illustrate the influence of temperature change to the diagnostic signals induced by changes in material properties (Sherrit *et al.*, 1999), (Brammer and Percival, 1970) the Lamb wave propagation is simulated for the described aluminum plate subjected to a temperature change of $75$ K.
For comprehensive parametric studies, material properties are selected as parameters. Sensor signals are simulated at $25^0$C, $50^0$C, and $75^0$C. Properties are varied individually to study the effect of each parameter

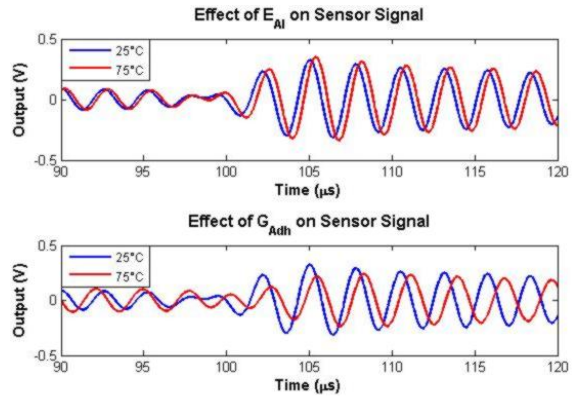


Figure 17: Numerical simulation of Lamb wave propagation in a thin aluminum plate subjected to different temperatures as environmental effect (upper: effect of changes in aluminum properties, lower: effect of changes in adhesive properties).

on the peak-to-peak amplitude and time of arrival of the sensor signal. The variation of adhesive stiffness can only be estimated and a $10$ % reduction in stiffness of adhesive for $25$ K rise in temperature has been assumed for the following parametric studies.

Figure 18 shows the percentage change in peak-to-peak amplitude and time of arrival for $100$, $300$ and $500$ kHz excitation frequencies (for a signal traveling between transducers both mounted with thick adhesive). Percentages are calculated based on signals at room temperature ( $25^0$C). Positive percentage values indicate an increase in peak-to-peak amplitude or time of arrival. From Figure 18 it can be concluded that major parameters affecting amplitude are adhesive shear modulus ($G_{\text{Adh}}$) and permittivity of PZT in thickness direction ($\varepsilon_{33}$). In the other hand, the major influence on time of arrival are given by the parameters of aluminum stiffness ($E_{\text{Al}}$), aluminum density ($\varrho_{\text{Al}}$), and adhesive shear modulus ($G_{\text{Adh}}$).
Figure 19 compiles experimental and simulation results. As can be seen, for higher temperatures the amplitude tends to decrease and delay of time arrival is obtained. Numerical simulations show good correlations with experiments in trends of both amplitude and arrival time. Discrepancies in experimental and simulation results are mainly due to uncertainty in variation of material properties with temperature.

In summary, the developed simulation technique is very promising to understand the physics behind the environmental influence to the propagation of Lamb waves. The presented study has shown the effects of temperature-dependent material properties to the wave propagation as one important environmental factor. In particular, the dynamic behavior is affected by the properties of adhesive layers, which has hardly been studied so far. The trends in experiments are simulated with SEM and explained based on the knowledge acquired from the parametric studies.

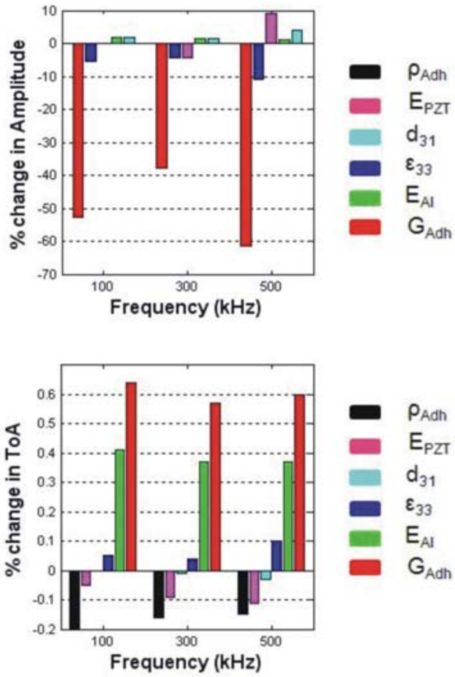


Figure 18: Parametric study on the influence of different temperature-induced parameter changes to propagation of Lamb waves (upper: peak-to-peak amplitude, lower: time of arrival (ToA)).

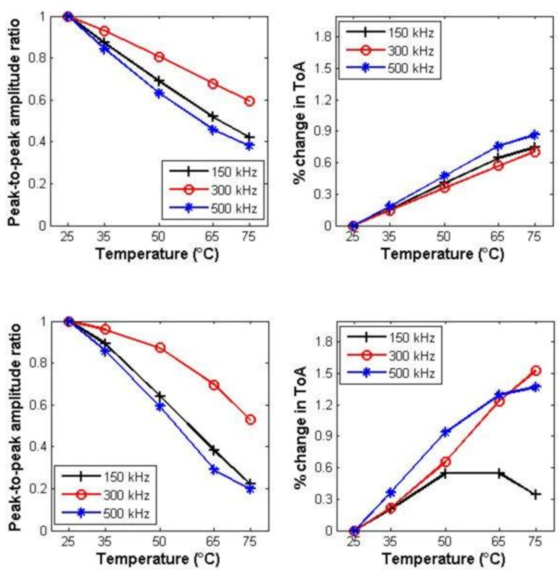


Figure 19: Comparison of experimental and numerical results on the influence of temperature effects to Lamb wave propagation (left: peak-to-peak amplitude, right: time of arrival, upper: simulation results, lower: experimental results).

## 6 OUTLOOK – PROGNOSIS OF REMAINING USEFUL LIFETIME

The current work focuses on the development of an appropriate technique for the prognosis of remaining useful lifetime of structures based on the outputs of damage diagnosis and prediction of impact-induced damage. In the following, the key steps of the proposed methodology will be primarily presented and discussed rather than extensive results. Furthermore, fundamental examples will provide basic validation of the procedure and will show the feasibility of the integrated lifetime prognosis.
There is a significant difference between Health Monitoring and Health Management. Health Management uses Health Monitoring to detect structural damage, then evaluates how the structure is affected by the damage (Prognostics – Residual strength) and estimates how long the structure can operate after this damage (Prognostics – Remaining useful lifetime). Accordingly, the strategy of the integrated system comprises that after damage diagnosis by the active sensing system, the current health status of the structure is submitted to the prognostic module to achieve certain prognostic information. In order to yield accurate predictions of damage growth and residual strength, one key issue is to create a proper link between the diagnostic outputs and prognostic inputs. This link can be broken down into four main modules. Currently, the authors are focusing on the diagnostic systems (as described above) and on the progressive failure analysis module. The remaining diagnostics / prognostics (DP) link modules, described in detail below, constitute the road map to be followed for the successful deployment of the proposed health management system. Figure 20 presents the flow of inputs and outputs within the different modules.

**A.) Health Data Transfer.** The goal of this step is to map the diagnosed damaged area to the structure's Finite Element model. The error in detection and extraction of health data can significantly affect the accuracy of the life-time prediction. Therefore, the extraction of health data from the diagnostic results is of immense importance.

**B.) Identification of Damage Mechanism.** Due to anisotropy of laminated composites there are different damage processes within the laminate: (1) Transverse Matrix-cracking, (2) Fiber-matrix debond (splitting), (3) Delamination, and (4) Fiber breakage. Depending on the loading situation one type of fracture will nucleate and progress to the others. Characterizing the diagnostic outputs with failure modes is crucial and future research need to be conducted to overcome these difficulties. The current approach is as follows. By collecting the data of degradation by damage diagnosis and determining or predicting the loading spectra during operation an estimate of the sustained damage type can be made. This running estimate of the damage accumulation can be recorded and reconciled with future results of damage diagnosis at less frequent intervals. With these estimates either damage tolerance or safe-life philosophy can be applied, as appropriate for the particular case, to estimate remaining useful lifetimes.

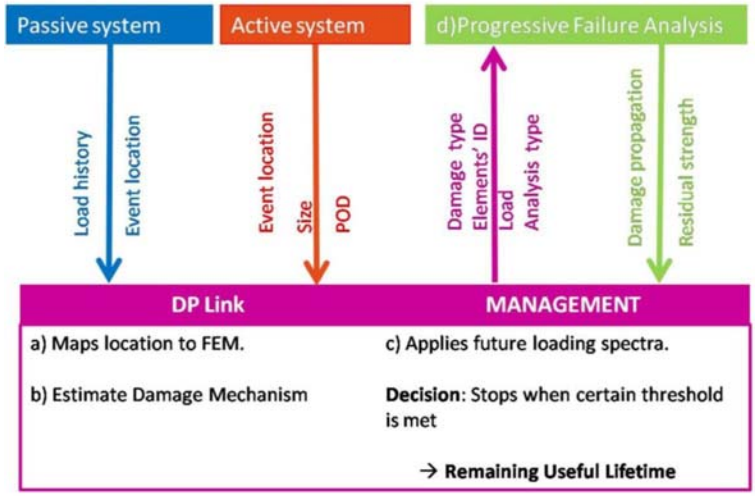


Figure 20: Flowchart of link from diagnostics to prognostics (DP link).

**C.) Management / Decision.** This module's objective is to provide the progressive damage analysis with a future loading scenario to estimate damage progression. These future load spectra can be either damage tolerance or safe-life philosophy. The damage tolerance approach assumes that a crack or flaw exists in a part and then determines the impact that a flight spectrum will have on the growth of the crack size. Safe-life methodologies are based on extensive service history and can determine the remaining lifetime of a part where no crack or flaw is expected to exist. By utilization of database techniques, an update of the RUL estimate after occurrence of a specified trigger event (i.e. impact) can be achieved near real-time and will be submitted to the decision-making module.

**D.) Progressive Failure Analysis.** The module of Progressive Failure Analysis evaluates structure performance and calculates a remaining life-time prediction given the current state of damage and future loading. A progressive failure analysis model, originally derived by Chang and his associates (e.g. (Chang and Qing, 1997)) for the simulation of damage in bolted composite joints, was adopted and extended. A Hashin-based failure criterion (Hashin, 1980) was selected to predict the damage during the evolution of load history. When the criterion is fulfilled damage is introduced or propagated. It accounts for matrix micro-cracking, and uses degradation factors to account for other damage mechanisms, while it does not predict delamination. Future work will focus on extending the analysis to include delamination following the methodology described in the previous sections. Upon damage the stiffness and strength of the laminate are degraded following a degradation model developed based on fracture mechanics (Shahid and Chang, 1993). The model was implemented as a user defined material constitutive model subroutine (UMAT) in the commercial Finite Element package ABAQUS/Standard.

The current modified version of the analysis accounts for low cycle fatigue loads using a ply based fracture mechanics approach that predicts matrix micro-cracking initiation and propagation. As has been described above, matrix micro-cracking is the initial cause of delamination (Choi, 1990), and therefore, an accurate prediction of matrix cracking is necessary prior to modeling delamination.
First, the traditional approach of low cycle fatigue growth was implemented (Harris, 2003), (Nairm, 1999) using Paris Law. In order to validate the algorithm, results of the numerical analysis were compared to published experimental data (Lafarie-Fernot *et al.*, 2001), (Nairm, 1999). As can be seen from Figure 23, the traditional approach results follow the experimental trend. Still there are significant differences between experiment results and numerical analysis mainly caused by uncertainty in material properties. Performing according experiments for material characterization may be time consuming and costly, even with a view that the relationships stated above are dependent on many parameters such as frequency, load ratio and laminate configuration.

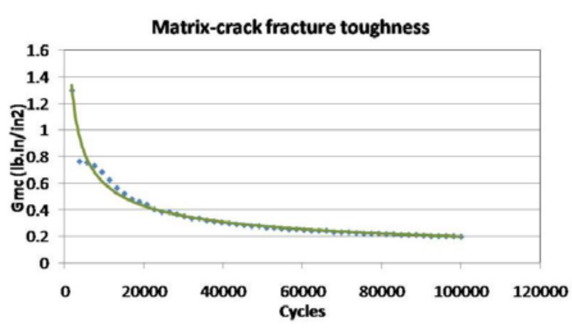


Figure 21: Degradation of matrix-crack fracture toughness $G_{mc}$ with increasing number of cycles (blue dots: data points, green line: curve fit).

In order to increase the robustness and efficiency of the proposed fatigue analysis a new approach was developed and implemented. The main assumptions of the new formulation will be discussed briefly in the following. The current damage approach uses the ply based material degradation model previously developed by (Shahid and Chang, 1993). This model considers the value of ply matrix-crack fracture toughness $G_{mc}$ as a limit for crack initiation. Traditionally, the value of $G_{mc}$ is assumed being constant under static loading conditions. In order to account for the fatigue loading problem, the matrix-crack fracture toughness $G_{mc}$ is introduced here as function of the cycles $G_{mc} = G_{mc}(N)$. The value of $G_{mc}$ will degrade with increasing number of cycles as shown in Figure 21. The degradation function for the fracture toughness $G_{mc}$ shown by Figure 21 represents preliminary data and has been obtained from back-calculating the matrix-crack fracture toughness from the traditional approach results. Finally, a preliminary empirical relationship was computed by a curve fit of this data.
Equation 6 shows the mathematical representation of the matrix-crack fracture toughness $G_{mc}$ as a function of load cycles

$$G_{mc} = A\,N^{\eta} \tag{6}$$

where $N$ denotes the number of cycles and $A$, $\eta$ are material constants. This empirical relationship can be measured using slightly modified standard fracture toughness testing methods (Nairm, 1999), which are the subject of future experiments. By introducing $G_{mc}$ as a function of cycles, the material degradation model is now dependent on the number of accumulated cycles $N$, and accordingly the ply strengths are updated after each loading cycle. After each update of the strengths a modified Hashin strength criterion is evaluated and damage will propagate if the criterion is fulfilled. Figure 22 illustrates the major steps of the algorithm used in the current analysis as described.

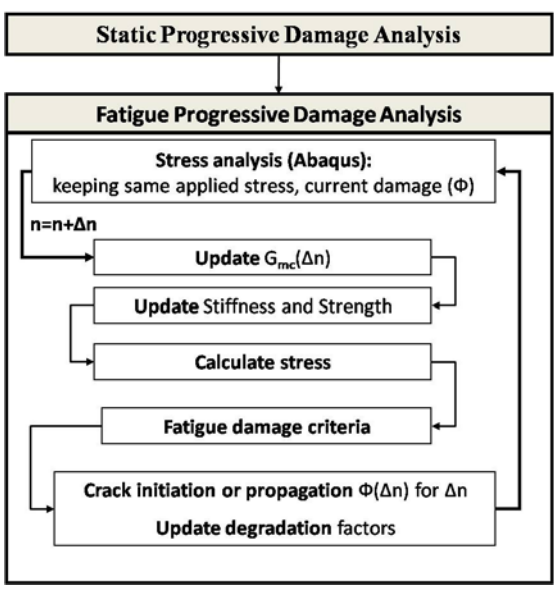


Figure 22: Algorithm used for the UMAT/Abaqus progressive Finite Element analysis.

In order to validate the proposed algorithm, results of the numerical analysis for both the traditional approach using Paris Law and the new approach were compared with published experimental data (Lafarie-Fernot *et al.*, 2001), (Nairm, 1999). The example presented here is a T300/914 (and T300/934) $[0_4/90/0_3]_S$ laminate subjected to tension-tension low cycle loading. The first step was to perform the static analysis to acquire the static failure load. Once this load was known, the cyclic load was set to eighty percent of the static failure load.
As can be seen from Figure 23, the results of the new approach clearly give a better representation of the experimental results and follow the experimental trend very well. Even though there is still room for further improvement, the current analysis helps us to understand and to characterize damage propagation and strength degradation for composites. Additionally, it provides a preliminary tool to develop the DP link modules as a major part of the near-future work.

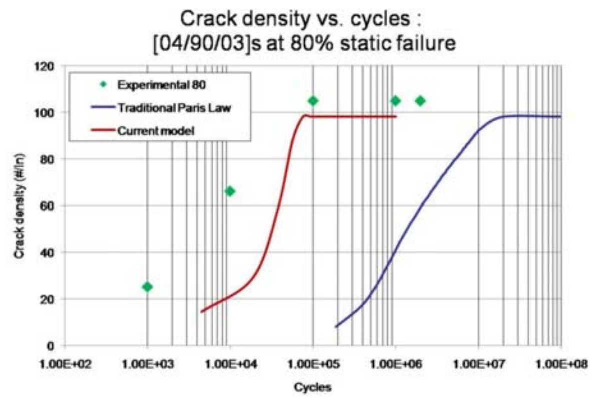


Figure 23: Comparison of numerical and experimental results for fatigue analysis; material properties based on T300/914 (and T300/934).

## 7 CONCLUSIONS

Next generation health management technology will link different key technologies as impact monitoring by passive sensing, numerical prediction of impact-induced damage, diagnosis of structural damage by active sensing, and prognostics of remaining useful lifetime to an interactive system for integrated vehicle health management. One of the striking features of the proposed system is the continuous exchange of health data between the different subsystems to update the structural models and to feed the real-time automated reasoning and decision making systems with various health data.
The contribution has reported the current state of the development of an interactive health management system in terms of system design, basic functionalities of the single SHM subsystems and data exchange between the modules. Some typical examples have demonstrated the fundamental capabilities of the proposed health management system and open questions as well as future needs and developments have been discussed.

In summary, the following capabilities are merged within a unique system for integrated vehicle health management:

1. Both impact location and impact force history can be identified in real-time by impact monitoring based on passive sensing data. An automated procedure for system calibration will be implemented.
2. The impact characteristics will be submitted subsequently to a damage prediction module to estimate the occurrence and severity of impact-induced damage.
3. After an adverse event, active diagnosis is performed to acquire the current health status of the structure. Environmental effects on the diagnosis results are compensated by updated baseline data. For this purpose, the propagation of diagnostic waves under environmental conditions is simulated and evaluated.
4. Health data from active sensing is passed to the prognostics module where numerical simulation of progressive failure under future load conditions is performed. The remaining useful lifetime will be estimated by consideration of an allowable damage/degradation limit.
5. A global health management interface controls the system and data flow interactively and provides real-time reasoning and decision-making capabilities.

## ACKNOWLEDGMENTS

The authors would like to acknowledge the National Aeronautics and Space Administration (NASA) for the support of this work under grants NRA-07-IVHM1-07-0061 and NRA-07-IVHM1-07-0064. In particular, we would like to thank Richard W. Ross (NASA LaRC) as the program monitor for his support of the project. Furthermore, the authors are grateful for collaboration with Honeywell Inc. and Acellent Technologies. In particular, the authors acknowledge Acellent's contribution and assistance on the passive and active sensing systems.

## REFERENCES

(Boller *et al.*, 2009) C. Boller, F.-K. Chang, and Y. Fujino (Eds.). Encyclopedia of structural health monitoring. In *John Wiley & Sons*, 2009.

(Brammer and Percival, 1970) J. A. Brammer and C. M. Percival. Elevated-temperature elastic moduli of 2024 aluminum obtained by a laser-pulse technique. *Experimental Mechanics*, 10(6):245–250, 1970.

(Chang and Beard, 1997) F.-K. Chang and S. Beard. Active damage detection in filament wound composite tubes using built-in sensors and actuators. *Journal of Intelligent Material, Systems and Structures*, 8:891–897, 1997.

(Chang and Ihn, 2004) F.-K. Chang and J.-B. Ihn. Detection and monitoring of hidden fatigue crack growth using a built-in piezoelectric sensor/actuator network: Part ii: validation through riveted joints and repair patches. *In C. T. Sun et al (editors), ASME - AD*, pages 621–630, 2004.

(Chang and Qing, 1997) F.-K. Chang and X. L. Qing. Recent advances in structural joints and repairs for composite materials. In *Edited by L. Tong and C. Soutis, Kluwer Academic Publisher*, pages 101–140, 1997.

(Chang and Roh, 1995) F.-K. Chang and Y. Roh. Effect of impact damage on lamb wave propagation in laminated composite structures. *In C. T. Sun et al (editors), ASME - AD*, 46:127–138, 1995.

(Chang and Seydel, 2001) F.-K. Chang and R. E. Seydel. Impact identification of stiffened composite panels: Part i: system developments. In *Smart Materials Structures. Institute of Physics Publishing*, 2001.

(Chang *et al.*, 2008) F.-K. Chang, I. Mueller, and K. Lonkar. Integrated passive-active interactive diagnostic technique based on efficient inverse methods for condition monitoring and damage detection for an integrated vehicle health management. In *Annual Report to National Aeronautics and Space Administration (NASA), Department of Aeronautics and Astronautics, Stanford University*, 2008.

(Choi, 1990) H. Choi. Damage in graphite/epoxy laminated composites due to low-velocity impact. In *Dissertation, Department of Aeronautics and Astronautics, Stanford University*, 1990.

(Doyle, 1987) J. F. Doyle. Experimentally determining the contact force during the transverse impact on an orthptropic plate. *Journal of Sound and Vibration*, 118:441–448, 1987.

(Fogg *et al.*, 1993) B. R. Fogg, M. F. Gunther, and A. Wang. Fiber optic impact detection and location system embedded in a composite material. In *Proceedings of SPIE Conference*, pages 262–269, 1993.

(Geubelle and Baylor, 1988) P. H. Geubelle and J. S. Baylor. Impact-induced de-lamination of composites: a 2d simulation. *Composites, Part B*, 29B:589–602, 1988.

(Ha *et al.*, 2009) S. Ha, A. Mittal, K. Lonkar, and F.-K. Chang. Adhesive layer effects on temperature-sensitive lamb waves induced by surface-mounted pzt actuators. In *Proceedings of 7th International Workshop on Structural Health Monitoring, Stanford CA*, pages 2221–2233, 2009.

(Hadamard, 1923) J. Hadamard. Lectures on the cauchy problem in linear partial differential equations. In *University Press, New Haven*, 1923.

(Harris, 2003) B. Harris. Fatigue in composites. In *Woodhead Publishing*, 2003.

(Hashin, 1980) Z. Hashin. Failure criteria for unidirectional fiber composites. *Journal of Applied Mechanics*, 47:329–334, 1980.

(Jiang *et al.*, 1998) Y. P. Jiang, K. Chandrashekara, and A. C. Okafor. Estimation of contact force on composite plates using impact induced strain and neural network. *Composites Part B: Engineering*, 29(4):363–370, 1998.

(Kim *et al.*, 2008) Y. Kim, S. Ha, and F.-K. Chang. Time-domain spectral element method for built-in piezoelectric-actuator-induced lamb wave propagation analysis. *AIAA Journal*, 46:591–600, 2008.

(Komatitsch and Vilotte, 1998) D. Komatitsch and J.P. Vilotte. The spectral element method: An efficient tool to simulate the seismic response of 2d and 3d geological structures. *Bulletin of the Seismological Society of America*, 88:368–392, 1998.

(Lafarie-Fernot *et al.*, 2001) M. C. Lafarie-Fernot, C. Henaff-Gardin, and D. Gamby. Matrix cracking induced by cyclic ply stresses in composite laminates. *Composites Science and Technology*, 61:2327–2336, 2001.

(Lessard, 1989) L. B. Lessard. Compression failure in laminated composites containing an open hole. In *Dissertation, Department of Aeronautics and Astronautics, Stanford University*, 1989.

(Ljung, 1999) L. Ljung. System identification – theory for the user. In *PTR Prentice Hall, 2nd edition*, 1999.

(Markmiller, 2007) J. Markmiller. Quantification and optimization of a structural health monitoring system for impact detection in composite structures. In *Dissertation, Department of Aeronautics and Astronautics, Stanford University*, 2007.

(Mueller and Chang, 2009) I. Mueller and F.-K. Chang. Model-based impact monitoring by inverse methods using particle swarm optimization. In *Proceedings of IMAC XXVII*, 2009.

(Nairm, 1999) J. A. Nairm. Applications of finite fracture mechanics for predicting fracture events in composites. In *5th International Conference on Deformation and Fracture of Composites, London UK*, 1999.

(Park and Chang, 2003) J. Park and F.-K. Chang. Built-in detection of impact damage in multiyayered thick composite structures. In *Proceedings of 4th International Workshop on Structural Health Monitoring, Stanford CA*, pages 1391–1398, 2003.

(Park, 2005) J. Park. Impact identification in structures using a sensor network: The system identification approach. In *Dissertation, Department of Aeronautics and Astronautics, Stanford University*, 2005.

(Raghavan and Cesnik, 2008) A. Raghavan and C. E.S. Cesnik. Effects of elevated temperature on guided-wave structural health monitoring. *Journal of Intelligent Material Systems and Structures*, 19(12):1383–1398, 2008.

(Scalea and Salamone, 2009) F. Lanza Di Scalea and S. Salamone. Temperature effects in ultrasonic lamb wave structural health monitoring systems. *The Journal of the Acoustical Society of America*, 124(1):161–174, 2009.

(Seydel and Chang, 1999) R. E. Seydel and F.-K. Chang. Implementation of a real-time impact identification technique for stiffened composite panels. In *Proceedings of 2nd International Workshop on Structural Health Monitoring, Stanford CA*, 1999.

(Shahid and Chang, 1993) I. Shahid and F.-K. Chang. Progressive failure analysis of laminated composites subjected to in-plane and shear loads. In *Department of Aeronautics and Astronautics, Stanford University*, 1993.

(Sherrit *et al.*, 1999) S. Sherrit, G. Yang, H. D. Wiederick, and B. K. Mukherjee. Temperature dependence of the dielectric, elastic and piezoelectric material constants of lead zirconate titanate ceramics. In *Proceedings of Intinternation Conference on Smart Materials, Structures and Systems, Bangalore, India*, 1999.

(Su *et al.*, 2006) Z. Su, L. Ye, and Y. Lu. Guided lamb waves for identification of damage in composite structures: A review. *Journal of Sound and Vibration*, 295:753–780, 2006.

(Wang and Chang, 2000) C. Wang and F.-K. Chang. Diagnosis of impact damage in composite structures with built-in piezoelectric network. *Proceedings of Smart Structures and Materials*, 3990:13–19, 2000.

(Wu and Chang, 1989) H.-Y. T. Wu and F.-K. Chang. Transient dynamic analysis of laminated composite plates subjected to transverse impact. *Computers and Structures*, 31(3):453–466, 1989.

(Wu and Springer, 1988) H.-Y. T. Wu and G. S. Springer. Impact induces stresses, strains and delaminations in composite plates. *Journal of Composite Materials*, 22:533–560, 1988.

(Yen *et al.*, 1994) C. S. Yen, E. Wu, and J. C. Yeh. Identification of impact forces at multiple locations on laminated plates. *AIAA Journal*, 32:2433–2439, 1994.